Simulation and Modelling of Dye-Sensitized Solar Cells Using MATLAB/Simulink

Ayodele O. Soge*, Boluwatife E. Adewoye, Oluwaseyi A. Ilori, Alexander A. Willoughby

Department of Physical Sciences, Faculty of Natural Sciences, Redeemer's University, PMB 230, Ede, 232102, Osun State, Nigeria

***Corresponding Author**

DOI: https://doi.org/10.51584/IJRIAS.2026.110400090

Received: 11 April 2026; Accepted: 16 April 2026; Published: 09 May 2026

ABSTRACT

This paper presents the modelling and simulation of electrical parameters of dye-sensitized solar cells (DSSCs) utilising MATLAB/Simulink. An equivalent single-diode circuit model was developed to represent the physical parameters influencing electron dynamics within the DSSC. The absorption coefficients of three natural dyes extracted with acetone were analyzed: *Vernonia amygdalina* (VAA), *Geoppertia macrosepala* (GMA), and *Cnestis ferruginea* (CFA). These coefficients were determined from existing UV-Vis analysis data. The model simulated the I-V and P-V characteristics of DSSCs sensitized with natural dyes across varying temperatures (275 - 325 K) and solar irradiance (320 - 1000 W/m²). Results indicated temperature increases slightly to enhance voltage output, while higher solar irradiance significantly boosts current across all dyes. Comparative analysis showed that dyes with higher absorption coefficients, such as GMA and VAA, produced greater current and power outputs than CFA. The model's validity was confirmed through experimental data, with minor discrepancies attributed to lower operating temperatures and greater TiO_2-layer thickness in the experimental setup. A functional DSSC solar panel comprising 500 GMA-sensitized cells was designed, achieving a maximum output of approximately 0.01 W. This research provides an effective MATLAB/Simulink model for predicting the performance of DSSCs with natural dyes and enhances understanding and optimization prior to fabrication.

Keywords: Renewable energy, Dye Sensitized Solar Cell (DSSC), MATLAB/Simulink, Absorption coefficient, Solar irradiance

INTRODUCTION

The growing global demand for energy and concerns for the environment caused by the long-term use of fossil fuels have intensified the search for sustainable renewable energy sources. Solar energy is abundant and clean, so it continues to stand out as an excellent alternative, and scientists are still making further improvements in the technologies used to harness it [1] [2]. The Dye-Sensitized Solar Cell (DSSC) is gaining significant attention among the various photovoltaic technologies being researched today. This new technology stands out because it is cost effective, easy to fabricate and can operate at a relatively higher efficiency even under reduced solar irradiance compared to the typical silicon solar cells [3] [4]. The way DSSCs operate is also very different. Unlike direct excitation of electrons in silicon cells, DSSCs behave more like a photoelectrochemical (PEC) system, a system that converts solar energy to electrical energy by triggering chemical reactions for the movement of electrons and other materials [1] [5].

The components of DSSCs are flexible substrates that are inexpensive and use a variety of transparent and lightweight materials. This gives manufactures flexibility in their design making them suitable for a wide range of applications, from building-integrated photovoltaics (BIPV) to powering small portable electronic devices [6]. Unlike traditional silicon solar cells, widely used and known for having a high-power conversion efficiency (PCE) between 18-22% [7], which involves energy-intensive processes, costly components, and is time-consuming. Due to the solid semiconductor that silicon cells require, their application in small and flexible

ISSN No. 2454-6194 | DOI: 10.51584/IJRIAS |Volume XI Issue IV April 2026

electronic devices is limited [8]. Additionally, most silicon solar cells have a lifespan of about 10 years and are often discarded in landfills after expiration due to little to no recycling options. This raises concern about their long-term sustainability as toxic metals like lead and cadmium used in manufacturing the cells, leaks and accumulates in the environment and would have a huge negative impact on the environment on the long run.

DSSCs typically consist of a natural or artificial dye coated on the surface of a semiconductor layer on a conductive glass, so that the dye molecules can absorb sunlight and inject electrons directly into the conduction band of the semiconductor [9] [10], while silicon-based solar cells absorbs sunlight and knock off electrons from the conduction band of the semiconductor itself, the electrons are then free to move around. This distinctive operation of DSSCs opens up possibilities for researchers to develop models that will accurately represent the electrical behaviour of the DSSCs and also help in analyzing the effect of different factors and materials to enhance the efficiency of the cells for better performance [6] [11].

Moreover, DSSCs have significantly evolved since they originated from basic laboratory experiments and are now being researched as a viable and more affordable alternative to conventional silicon cells, most especially for niche applications [12]. Although small fabricated cells have reached a power conversion efficiency (PCE) of over 14% [2] [13], they are not designed to compete directly with silicon cells but are more valued for the unique advantages that make them stand out. One of the most marketable applications of DSSCs is their excellent performance under indoor and low-light conditions. DSSCs are not as negatively impacted by artificial or scattered light as silicon cells are, explains [14]. This intrinsic quality places them as an ideal device to charge small electronic equipment. Imagine a day when Internet of Things (IoT) devices, wireless sensors, calculators, smart tags, and even wearable gadgets that charge themselves operate without the necessity of traditional batteries [15]. This ability to scavenge energy from ambient light is truly a battery-free solution for low-power devices, effectively eliminating repeated battery replacement needs, a fact noted by [16].

Besides facilitating small electronics, DSSCs are now being utilized on an increasing scale in building-integrated photovoltaics (BIPV). Being transparent, visually appealing, and having the potential to be produced in a vast array of colors and shapes, they are highly suited for simple integration into architectural elements like windows and skylights [2] [17]. This would mean that buildings could potentially generate electricity with DSSCs, without compromising on design freedom and allowing natural light to filter through [3]. Already, several companies are at the forefront of developing BIPV technology through DSSCs, transforming architecture into energy-producing assets [6].

Furthermore, the low cost of production and simple fabrication processes, typically compatible with efficient roll-to-roll printing techniques, positions DSSCs as a viable option for the fabrication of large-area, flexible, and customized energy solutions [12]. As DSSCs are opening doors to novel applications in intelligent fabrics, flexible screens, and potentially even large-scale outdoor installations, solving the instability and efficiency problems remain the utmost priorities for their widespread adoption [18]. Continuous research on new materials as well as investigation into their performance for enhanced stability will be crucial to expand their commercialization.

Ongoing research on DSSCs aims to optimize materials and structures, with a recent emphasis on simulative modeling for efficient and cost-effective understanding of electrochemical reactions and performance prediction. Software like MATLAB is instrumental in simulating P-V and I-V characteristics, energy band levels, and electrical responses of DSSCs across diverse environmental and material conditions [8] [19]. For example, Aboulouard et al. [20] assessed DSSC performance using natural dyes from Moroccan olive leaves and red hibiscus flowers. A MATLAB-based simulation employing the electron diffusion model compared the photovoltaic efficiency of the two dyes. The olive leaf dye exhibited a superior and broader absorption spectrum compared to the red hibiscus, as evidenced by UV-Vis spectrophotometry. Additionally, the olive leaf dye demonstrated enhanced cell performance. The findings indicated that DSSCs dyed with olive leaf produced higher maximum power output, open-circuit voltage, and short-circuit current density. This research underscores the viability of using locally sourced plant dyes as a cost-effective and environmentally friendly option for dye-sensitized solar cells.

ISSN No. 2454-6194 | DOI: 10.51584/IJRIAS |Volume XI Issue IV April 2026

Furthermore, the study by Arumugam *et al*. [21] investigated the performance of dye-sensitized solar cells (DSSCs) with mesoporous zinc oxide (ZnO) as the photoanode layer and natural dyes as sensitizers using COMSOL Multiphysics software. The study also examined how various photoanode thicknesses and absorption coefficients were affected by the use of different dyes like anthocyanin, betalain, and chlorophyll. An optimum photoanode thickness of 600 nm was reported for ZnO-based DSSCs. The solar cell delivered a maximum power output of 0.309 μW with an efficiency of 12.4% using synthetic N719 dye. Amongst the natural plant dyes investigated, betalain delivered a higher efficiency due to its higher absorption coefficient. According to the authors, the usage of mesoporous ZnO as a photoanode in DSSCs can compete with TiO_2 while delivering a high efficiency with a lower cost for the material.

Atia and Ahmed [18] applied two mathematical modeling approaches – the single-diode and differential diffusion models – to reduce the cost of production and production time for DSSCs. Six optimization algorithms inspired by nature (for example, genetic algorithm, grey wolf optimization, and whale optimization) were utilized to identify the optimum physical parameters such as electron lifetime, electrode thickness, absorption coefficient, and diffusion coefficient, for the DSSC. An electron lifetime of 100 ms and a photoanode thickness of 1 μm, which collectively led to a predicted maximum DSSC efficiency of 11.79% were identified as the best design parameters. All six algorithms had good computational efficiency with convergence in a period within less than 20 times. In the study, a sensitivity analysis also emerged with the finding that environmental conditions were impactful on the short-circuit current density, open-circuit voltage, fill factor, and overall efficiency of the DSSC.

Tajvar *et al.* [22] utilized MATLAB for modeling and simulating natural dye-sensitized solar cells (DSSCs) to enhance understanding and optimization. Their research emphasized the potential of natural dyes as eco-friendly alternatives, focusing on a diffusion model to analyze the electrical properties of DSSCs. The study examined DSSCs sensitized with pomegranate, beetroot, and synthetic N-719 dyes. Through MATLAB simulations, the research assessed the influence of varying irradiance levels on the P-V and J-V characteristics of each cell. Findings indicated that electrode voltage increased with higher radiation due to elevated electron density. Additionally, the research explored the impact of the oxide layer thickness on the photoanode's performance and efficiency. Results demonstrated a reduction in short-circuit current and an increase in open-circuit voltage with thicker TiO2 electrodes.

Ogabi et al. [23] investigated the feasibility of natural dyes from Lagerstroemia speciosa flowers and leaves as sensitizers in DSSCs, emphasizing performance through simulation. Addressing the cost and environmental concerns associated with artificial dyes, the study sought alternatives via computational modelling using MATLAB. A diffusion-based theoretical model simulated the photoelectrochemical characteristics of DSSCs. Key internal parameters such as diffusion coefficient, electron lifetime, absorption coefficient, and light flux were derived from established models. Both purified and raw dye samples were assessed for photovoltaic efficiency, with conclusions drawn from variations in absorbance, anthocyanin content, and dye purity. The study highlighted that purification improved the absorption coefficient by eliminating inhibitory molecules, thus facilitating electron transport within dyes. Additionally, the research elucidated the interplay between dye composition, light absorbance, and their collective impact on DSSC performance. However, it was noted that future simulations should incorporate additional factors, such as recombination losses and resistance in conductive substrates, for improved forecasting.

Olulope et al. [12] described the fabrication, design, and simulation of a functional dye-sensitized solar cell based on electrochemical photovoltaic principles relevant to DSSCs. The research aimed to evaluate the viability of DSSCs in resource-limited settings. Synthetic ruthenium dye and iodide-based electrolytes were chosen for their reliable performance in DSSC construction. Titanium dioxide (TiO_2) was utilized as the semiconductor for the photoanode, counter electrode, and transparent conducting oxide substrate. A significant component of the research involved testing the simulation's performance throughout an entire day to assess the impact of varying solar radiation intensities on the average emitted voltage. Panda et al. (2018) conducted a study that introduced a mathematical model and simulated the characteristics of dye-sensitized solar cells (DSSCs) using MATLAB. This study analyzed the effects of various parameters, including recombination rate, electron diffusion coefficient, and photoanode film thickness, on I-V characteristics while comparing it to the overall cell

performance. The research elucidated the interrelationship between internal characteristics of the DSSCs and the cell's overall functionality.

Roy and Srivastava [24] numerically computed dye-sensitized solar cells (DSSCs) using a finite element method (FEM) and conducted the computation in MATLAB. The study modeled open-circuit voltages as well as photogeneration rates, thus providing significant information in correspondence with the optical as well as electric procedures in the system. It includes the application of refined numerical schemes towards research work concerned with common physical procedures of dye-sensitized solar cells (DSSCs).

The performance of plant-based dye-sensitized DSSCs were assessed in a study by Supriyanto et al. [25]. Using a MATLAB/Simulink model, the study modeled DSSCs sensitized with different types of natural dyes (Tumeric, Coffee, a mixture of Tumeric and Coffee, *Phyllanthus Reticulatus Poir* plant*, Piper Crocatum* plant, and *Melaleuca leucadendra* plant). The I-V and P-V curve for the different dyes was plotted. The plots showed the effect of varying the temperature and solar irradiance of each cell. Among all the dyes tested, *Melaleuca leucadendra* showed the best performance and obtained an open-circuit voltage (V_{OC}) of 0.7882 V and a short-circuit current (I_{SC}) of 3.2 mA.

Despite the level of advancements in the simulation and modeling of DSSCs, quite a number of problems still remain. Modeling the complicated aspect of the optical, electrical, and electrochemical processes in DSSCs under various working conditions is still a key challenge. Current models fall short in how well they can forecast DSSC performance under various conditions or how well they can model the impact of material interfaces and defects [3] [26].

Future modelling and simulation of DSSC will likely involve the integration of novel materials, such as perovskites and quantum dots, into existing models [27]. Artificial intelligence, including recent machine learning techniques, can also be employed to develop even more precise and predictive models of DSSC performance [3]. Amongst the other research areas, are the ones required for developing models that can simulate the long-term stability, as well as degradability of DSSCs, which are amongst the important variables in the commercialization of DSSCs [10] [28]. Technological breakthroughs in computer software along with model procedures will continue to accelerate further the development and application of sim ulation techniques for DSSCs.

Moreover, despite substantial progress in DSSC fabrication and optimization of materials, full commercialization is still a long way off due to materials being constrained by stability, vulnerable to ambient conditions, and with complex internal dynamics. Optimization for further increased power conversion efficiencies (PCEs) is a concern. More recent developments have demonstrated DSSCs to potentially reach efficiencies up to 15.2% with standard test conditions; though, this is short of comparing to other photovoltaic technologies (PV) [9] [19]. Electrolyte instability and dye degradation are the main challenges to DSSC long-term operational stability and efficiency in DSSCs is highly dependent on dye, semiconductor, and electrolyte. Optimization of components involves large-scale experimentation. Most models utilized so far to model DSSC behavior either lack the in-depth physic of their structure or too rigid to allow new material interfaces and variable physical conditions to be incorporated into them [6].

Furthermore, there is no common simulation framework to interconnect the photochemical process of DSSCs and the electrical outputs in a quantifiable and modifiable way. Empirical trial-and-error methods for system optimization still predominate among engineers due to it being time-consuming and expensive [11]. While some works have proposed MATLAB/Simulink-based simulations [8] [19], these models often fail to represent the complete dynamic behaviour under load, temperature, and spectrum variations. Besides, there is a limited study of an experimentally validated MATLAB/Simulink model, effective for the series and parallel combinations of Dye-Sensitized Solar Cells sensitized with natural dyes, for accurate panel performance prediction and efficient commercialization. Hence, this study aims to develop and implement an effective MATLAB/Simulink model for simulating the electrical performance of DSSCs, enabling the analysis and accurate prediction of their performance parameters under various operating conditions. The application of the proposed Simulink/MATLAB in designing a functional DSSC solar panel was also investigated.

ISSN No. 2454-6194 | DOI: 10.51584/IJRIAS |Volume XI Issue IV April 2026

METHODOLOGY

Derivation of Equations of the DSSC Model

The equivalent equations for the DSSC model are crucial for modelling the electrical characteristics of a DSSC. These expressions capture the interplay of charge generation, transport, and recombination within the DSSC structure. The DSSC equations for I_{SC} and V_{OC} are notably more complex and physically detailed than typical simplified models for conventional solar cells. They explicitly incorporate parameters related to the unique charge transport and recombination mechanisms within the porous TiO_2 and dye layers, such as electron diffusion length (L), TiO_2 thickness (d), absorption coefficient (α), electron concentration (n_o), and diffusion coefficient (D).

Short-Circuit Current (I_{SC}): The equation for short-circuit current density represents the maximum current produced when the voltage across the cell is zero [25]:

$$I_{SC} = \frac{q\phi L\alpha}{1 - L^2\alpha^2}\left[-L\alpha + tanh\ tanh\left(\frac{d}{L}\right) + \frac{L\alpha e^{-d\alpha}}{cosh\ cosh\left(\frac{d}{L}\right)}\right] \quad (1)$$

where:

q= electron charge, the fundamental constant that represents the charge of a single electron and is the same value carried by an excited dye molecule.

Φ= sunlight intensity quantifies how much of the incident photons that the cell receives, and it directly influences the rate at which electron and hole pairs are generated.

L= length of electron diffusion. It reflects how far an electron can travel within the TiO_2 network before recombining. A longer diffusion length indicates more efficient charge collection.

d= length of TiO_2. It represents the thickness of the porous titanium dioxide semiconductor layer, which is crucial for dye loading and electron transport.

α= the absorption coefficient affects how strongly the dye absorbs photons, and at what peaks in the solar spectrum. It also affects the concentration of excited electrons.

The I_{SC} equation model contains exponential and hyperbolic terms, which emphasize the subtle interactions of photon absorption, electron injection, porous TiO_2 network diffusion, and recombination processes. This level of detail distinguishes it from more primitive I_{SC} models for conventional solar cells, which resort to direct proportionality to light intensity and quantum efficiency.

Open-Circuit Voltage (V_{OC}): The equation for the open-circuit voltage represents the maximum voltage across the cell when the current of the cell is zero, and it is given as [21]:

$$V_{OC} = \frac{kTm}{q}\ ln\left[\frac{LI_{SC}}{qDn_0\ tanh\ tanh\left(\frac{d}{L}\right)} + 1\right] \quad (2)$$

where:

k= Boltzmann constant.

T= temperature is significant, as it influences the open-circuit voltage. It increases the concentration of electrons moving the cell, thus increasing the saturation current.

ISSN No. 2454-6194 | DOI: 10.51584/IJRIAS |Volume XI Issue IV April 2026

m= the ideality factor shows how much recombination happens in the DSSC, and it relates to the ideal performance of the cell.

q= electron charge.

D= the diffusion coefficient quantifies the mobility of electrons within the TiO_2 film, and it affects how efficiently they reach the current collector.

n_0= the electron concentration represents the equilibrium electron concentration in the semiconductor, influencing the intrinsic properties of the device.

The V_{OC} equation is dependent on the light-generated current (I_{SC}) and various material-specific and recombination-related parameters. The term: $qDn_o\ tanh\ tanh\ \left(\frac{d}{L}\right)$, effectively represents the saturation current (I_o) or recombination current component, which is a primary determinant of V_{OC}. The Ideal factor, m, is usually significantly higher compared to the typical diode ideality factors (n = 1-2) observed in conventional silicon solar cells. The high value allows the model to account for dominant, highly non-ideal recombination pathways or complex charge transport phenomena within the DSSC. In semiconductor physics, a high ideality factor indicates that the current-voltage relationship deviates significantly from ideal diode characteristics, typically due to recombination processes that are more complex than simple diffusion. For DSSCs, where recombination at the TiO_2 layer and within the electrolyte are significant issues, this high m value is the model's way of capturing the complex, non-ideal loss mechanisms.

General Current (I) equation [29]:

$$I = I_{SC} - \frac{qDn_o}{L}\ tanh\ tanh\ \left(\frac{d}{L}\right)\left[exp\left(\frac{qV}{kTm} - 1\right)\right] \quad (3)$$

This equation is a modified one-diode model where **I_{SC}** acts as the light-generated current (**I_{ph}**).

The reverse saturation current (dark saturation current) of the DSSC is given as:

$$I_0 = qDn_o\ tanh\ tanh\ \left(\frac{d}{L}\right) \quad (4)$$

General Voltage (V) is the terminal voltage across the cell. This equation describes the entire current-voltage characteristic curve of the DSSC. It is used to determine the value of **I** for corresponding values of **V** [29]**.**

$$V = \frac{kTm}{q}\ ln\left[\frac{L(I_{SC} - I)}{qDn_o\ tanh\ tanh\ \left(\frac{d}{L}\right)} + 1\right] \quad (5)$$

The DSSC equation parameters and values are presented in Table 1.

Table 1. DSSC equation parameters and values

Symbol	Description	Value	Unit
K	Boltzmann constant	1.381×10^{-23}	J/K
q	Electron charge	1.602×10^{-19}	C
L	Length of electron diffusion	2.2361×10^{-3}	cm
d	Length of TiO_2(thickness of the TiO_2 glass)	10×10^{-4}	cm
α	Absorption coefficient	5000	cm^{-1}
m	Ideality factor	45	No Unit

ISSN No. 2454-6194 | DOI: 10.51584/IJRIAS |Volume XI Issue IV April 2026

D	Diffusion coefficient	5.0×10^{-4}	cm^2s^{-1}
n_0	Electron concentration	10×10^{16}	cm^{-3}
Φ	Sunlight intensity	1×10^{17}	$cm^{-2}s^{-1}$
T	Temperature	273-375	K

Implementation of DSSC Modelling in Simulink

The bulk of modeling the DSSC lies in expressing the derived equations for the DSSC in Simulink functional block diagrams. It required selective choosing and establishing of various mathematical and logical blocks available in the Simulink library. Partitioning the Simulink model into well-defined subsystems (e.g., for the I_{SC}, V_{OC}, and the implicit I-V equations) has the highest value with respect to controlling complexity in the DSSC equations. It significantly enhanced model readability and simplified debugging. It improved the reusability of components, which is especially beneficial when scaling the model to simulate DSSC arrays. All numerical values for the DSSC constants (k, q, L, d, α, m, D, n_o, Φ, T) are accurately entered into their respective constant blocks within the Simulink model. For enhanced flexibility and ease of modification, these parameters are defined as variables in the MATLAB workspace before running the simulation. This allowed for quick changes to environmental conditions (like sunlight intensity or temperature) or material properties without needing to open and edit individual blocks in the Simulink model.

The flow chart for the modelling and simulating DSSC in MATLAB/Simulink is illustrated in Fig. 1.

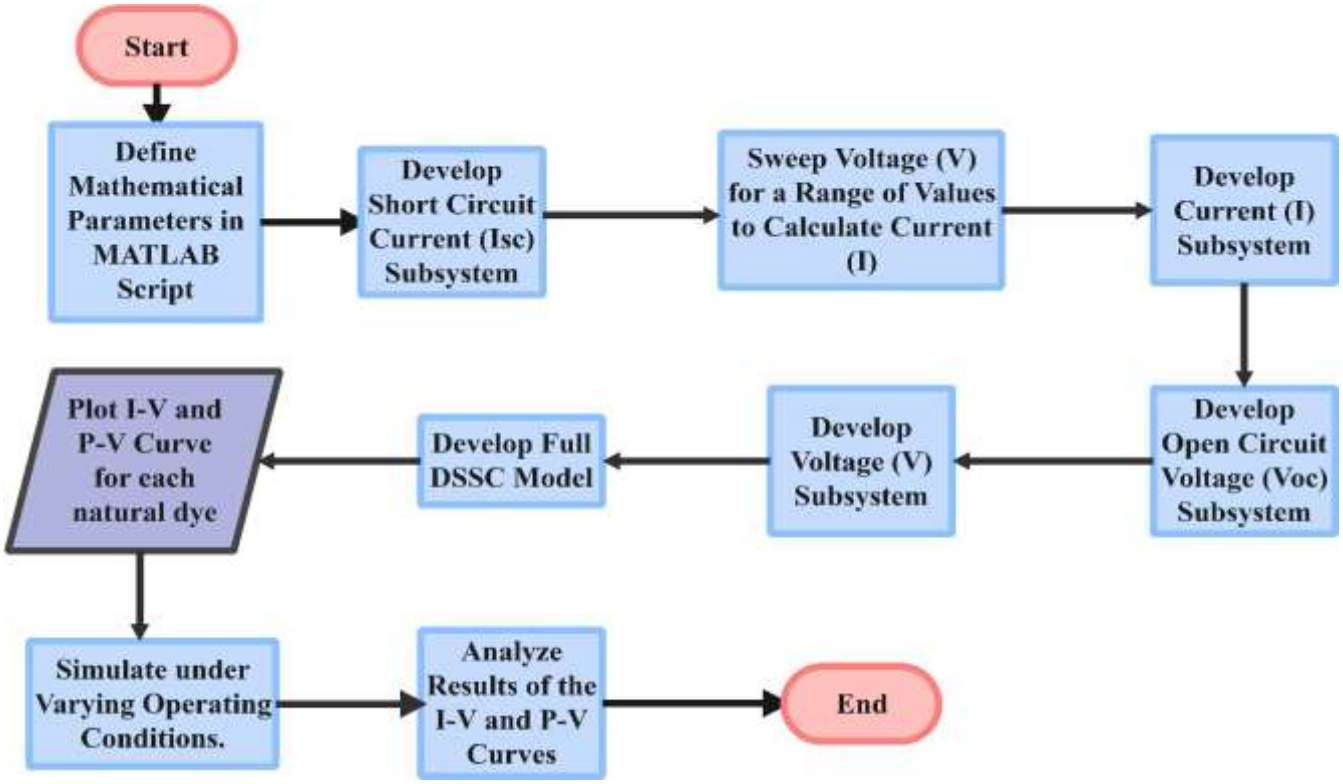

Figure 1. Flowchart of the Modelling and Simulation Process in MATLAB/Simulink

Essential Simulink Blocks and Their Application

A summary of the important Simulink blocks for the DSSC model implementation is presented in Table 2.

Table 2. Summary of Key Simulink Blocks for the DSSC Model Implementation

Block Name	Purpose of the DSSC Model	Simulink Library
Math Function	Implementing exponential, logarithm, and power operations	Math Operations
Trigonometric Function	Implementing hyperbolic tangent and hyperbolic cosine functions	Math Operations
Gain	Scaling parameters and coefficients	Math Operations

Sum	Performing addition and subtraction operations	Math Operations
Product	Performing multiplication operations	Math Operations
Divide	Performing division operations	Math Operations
Constant	Inputting fixed numerical parameters and constants	Sources
Scope	Visualizing simulation results (e.g., I-V curves, Isc, Voc)	Sinks
Algebraic Constraint	Solving implicit equations and resolving algebraic loops	Math Operations

Modular Design with Subsystems

To manage the complexity in the DSSC equations, it is also used in formulating the model in a modular fashion with separate subsystems for each important component:

i. Short-Circuit Current Subsystem: It contains all the blocks for computing the Short-Circuit Current (I_{SC}). It accepts the respective constants as input and gives the computed I_{SC} values (Fig. 2).

ii. Open-Circuit Voltage Subsystem: Open-Circuit Voltage (V_{OC}) Subsystem takes the value of I_{SC} calculated, along with the rest of the constants, as input, and gives the V_{OC} as an output (Fig. 3).

iii. I-V Characteristic Subsystem (Implicit): This is the most involved component due to the implicitness of the I-V equation, i.e., voltage and current are functions of one another. A set of voltage values was used to calculate the corresponding values of the current. This was achieved by using a Repeating Sequence block in generating a sweep of input currents to plot the entire I-V curve (Figs. 4 and 5).

The output terminals of the blocks were connected correctly with the input of the subsequent blocks with the direction of the signal flow watched so that all blocks were properly configured according to the mathematical equations and values of each parameter. The full DSSC model is displayed in Fig. 6.

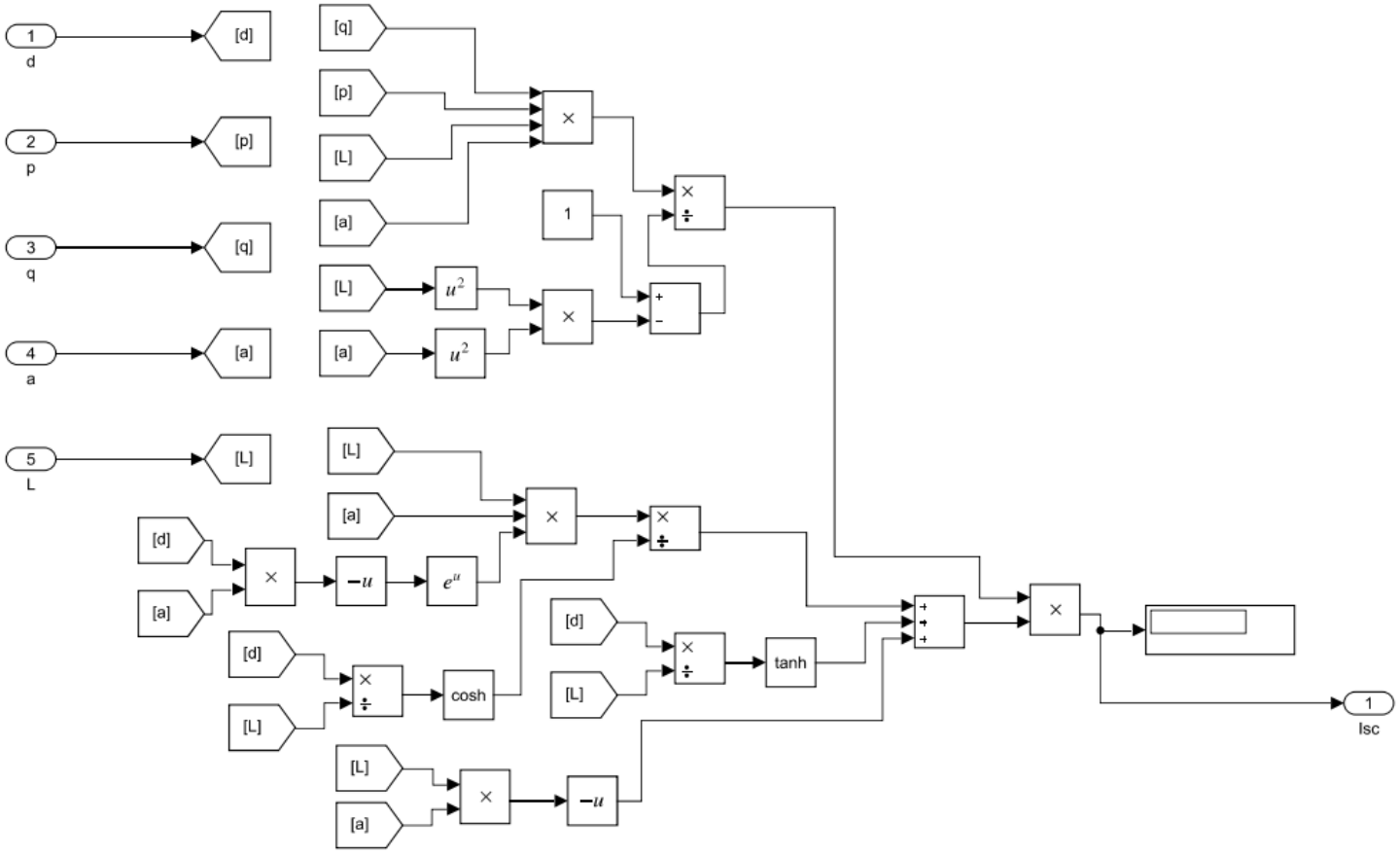

Figure 2. Short-Circuit Current Subsystem

ISSN No. 2454-6194 | DOI: 10.51584/IJRIAS |Volume XI Issue IV April 2026

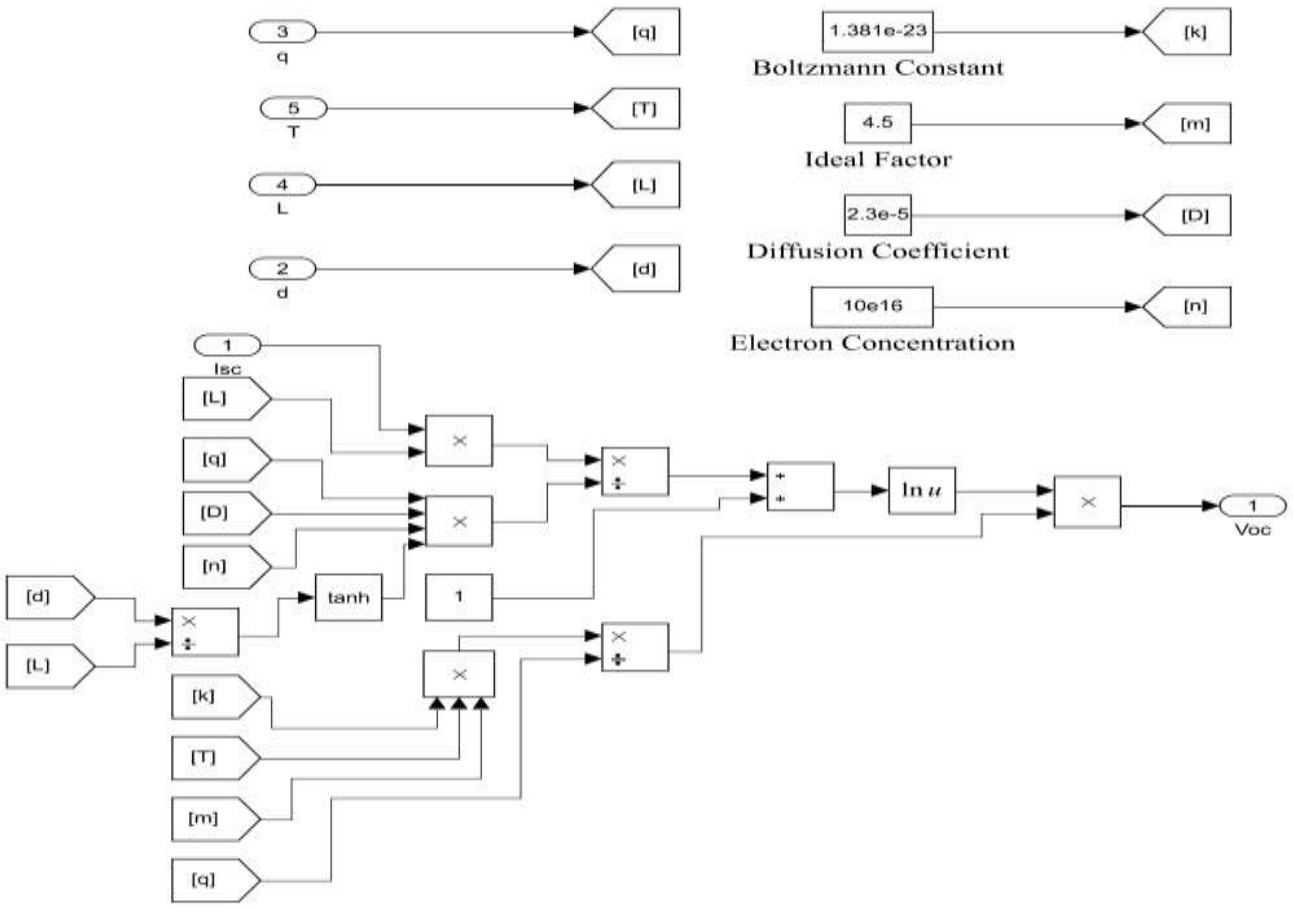

Figure 3. Open-Circuit Voltage Subsystem

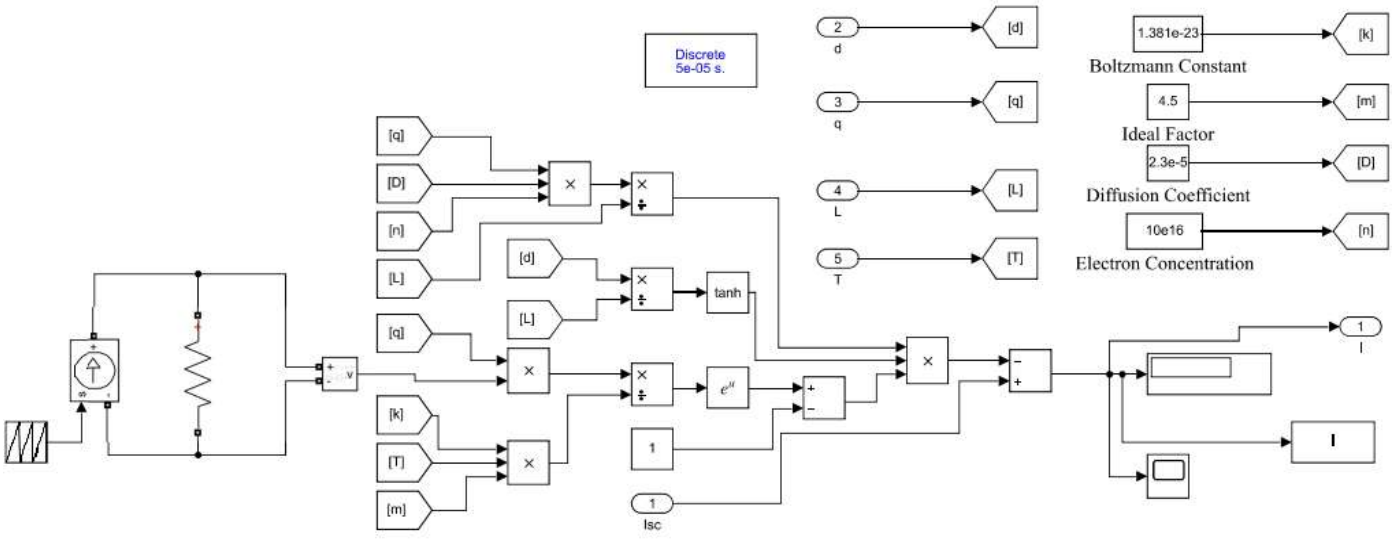

Figure 4. Current Subsystem

ISSN No. 2454-6194 | DOI: 10.51584/IJRIAS |Volume XI Issue IV April 2026

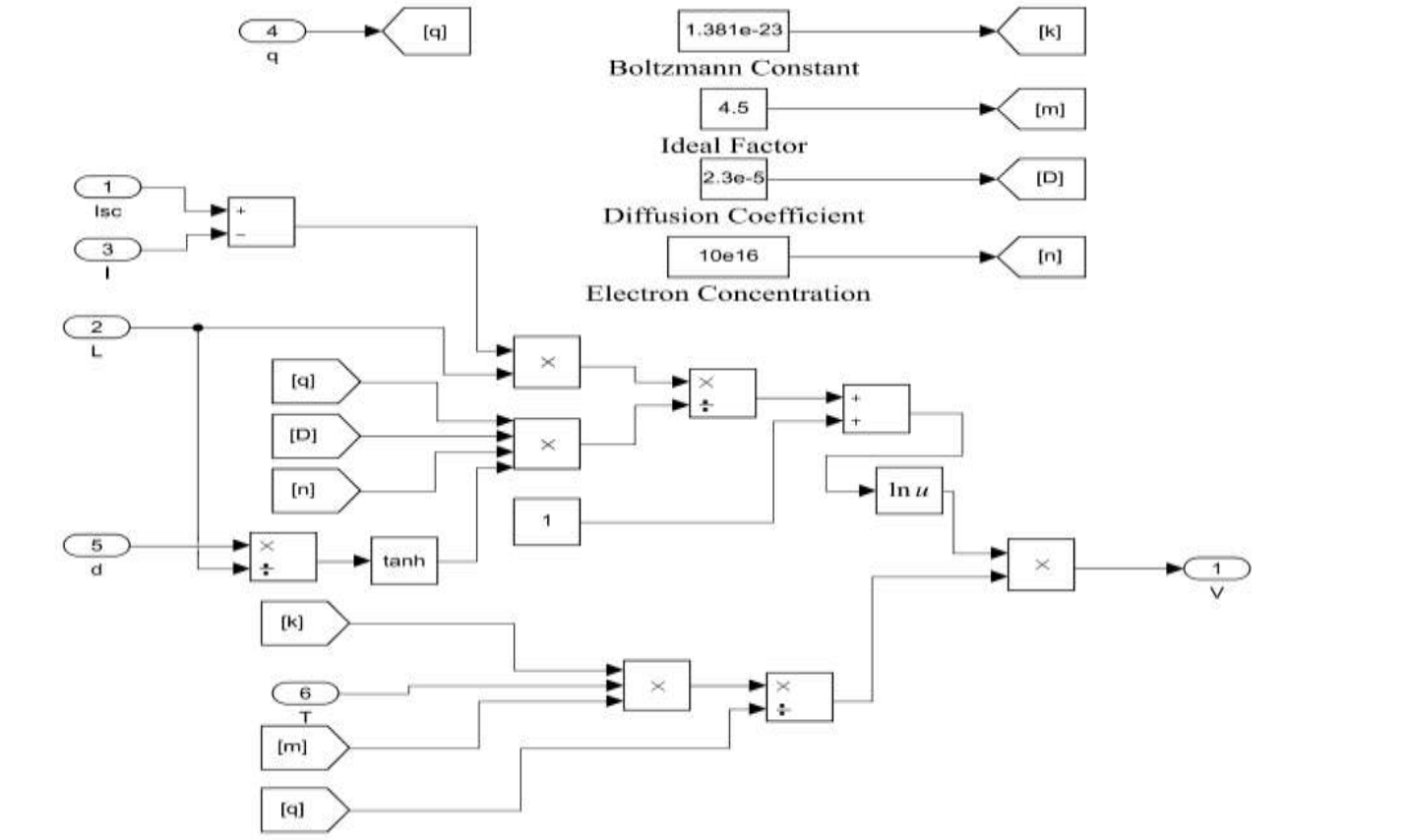

Figure 5. Voltage Subsystem

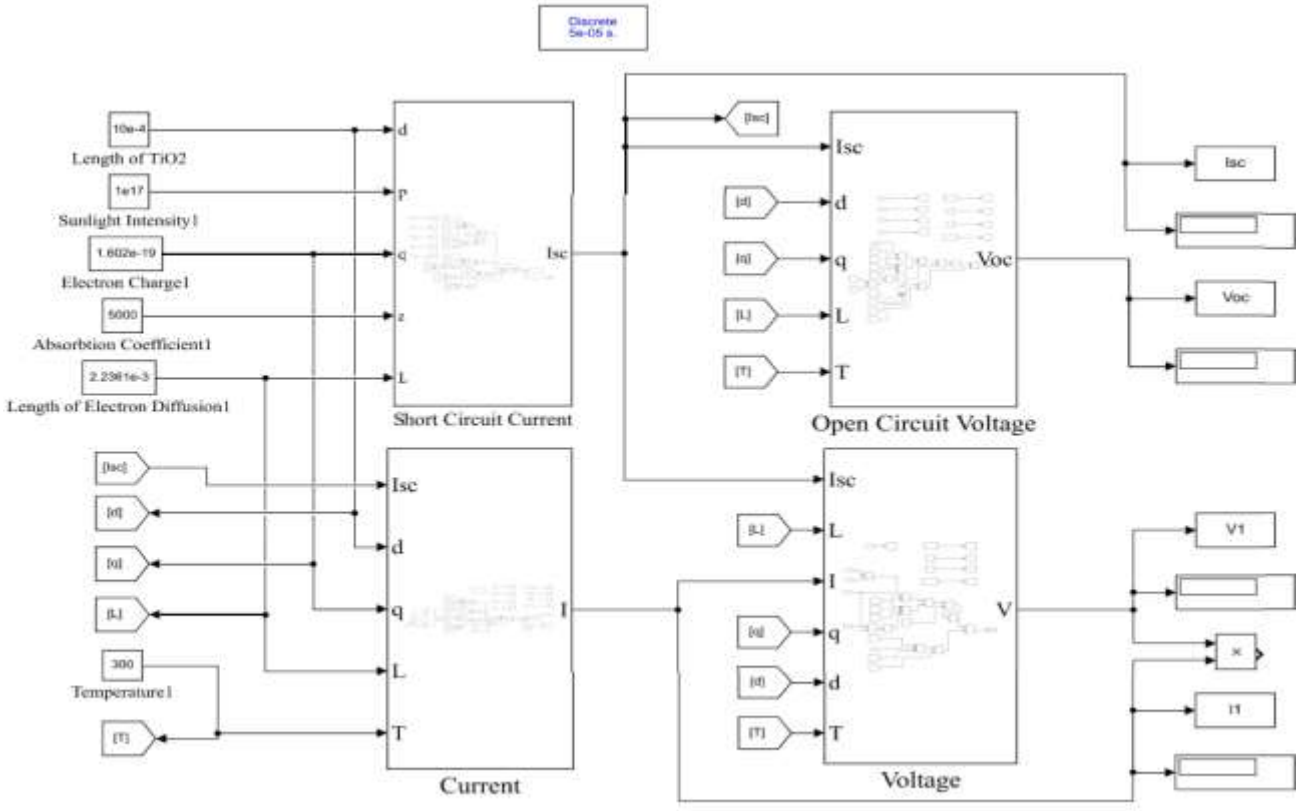

Figure 6. Full DSSC Model

ISSN No. 2454-6194 | DOI: 10.51584/IJRIAS |Volume XI Issue IV April 2026

RESULTS AND DISCUSSIONS

The simulation results derived from the MATLAB/Simulink model for DSSCs with three natural dye extracts of bitter leaf (*Vernonia amygdalina*), calathea (*Goeppertia macrosepala*) leaves, and wild alder (*Cnestis ferruginea*) fruit as photosensitizers are presented. Their P-V and I-V characteristics are displayed at different temperatures and irradiance.

Absorption Coefficient

Absorption coefficient is the intensity at which the dye absorbs light at a certain wavelength. In natural dyes, the absorption coefficient is wavelength, extraction solvent, concentration of the dye, and pH of the dye dependent. This is typically determined by the absorbance at the peaks of different wavelengths within the UV to visible range of light spectrum. UV-Vis analysis was performed on three natural dyes using a PerkinElmer Lambda 1050 spectrophotometer.

The absorption coefficient is calculated as expressed by Eq. (6) using the Beer-Lambert law, where the absorption coefficient is directly proportional to the absorbance [20].

$$\alpha = \frac{2.303 \times A}{d} \qquad (6)$$

where ***A*** is the absorbance (a.u) and ***d*** is the path length (or thickness) of the TiO_2 layer (in cm).

Simulation Results for Individual Dyes
Dye 1*:* Natural dye extract of bitter leaf *(V. amygdalina)* with acetone as solvent (VAA)

In the 500-600 nm visible light range, *V. amygdalina* (VAA) dye has a peak absorbance at 504, 536, 560 and 600 nm as reported in our previous work [4]. An average peak absorbance of 0.17 is considered, which falls near 550 nm in the centre of the visible light spectrum and represents the point where the DSSC would generate most of its current during peak sunlight. The absorption coefficient of the solar cell is estimated as 3900 cm^{-1} using Eq. (6). Figure 7 shows the current-voltage (I-V) characteristics of VAA-sensitized DSSC at a constant solar irradiance of 1000 W/m^2 across three temperatures: 275 K, 300 K, and 325 K. The curves indicate that as the temperature increases, the voltage also increases. At the same time, the current remains at a stable level of approximately 0.048 A.

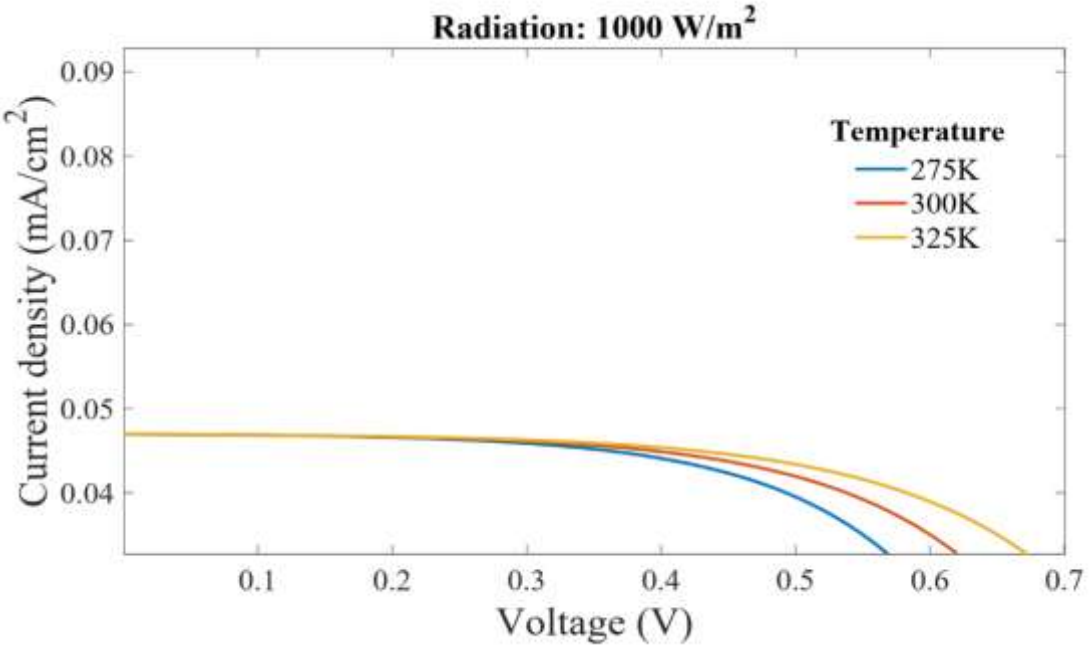

Figure 7. I-V Curve under varying temperatures and at a solar irradiance of 1,000 W/m^2 (VAA)

ISSN No. 2454-6194 | DOI: 10.51584/IJRIAS |Volume XI Issue IV April 2026

The curve for 325 K shows the highest voltage on the -axis. In comparison, the 275 K curve shows the lowest value, indicating a direct positive correlation between the operating temperature and the overall voltage output of the VAA-sensitized DSSC under these conditions.

Similarly, Figure 8 shows the current-voltage (I-V) characteristics of the VAA dye-sensitized solar cell at a constant temperature of 300 K across three different irradiance levels: 320 W/m², 640 W/m², and 1000 W/m². The curves demonstrate that as irradiance increases, the current increases significantly, and the voltage also increases. The curve for 1000 W/m^2 shows the highest current. It extends to the highest voltage on the x-axis. At the same time, the 320 W/m^2 curve shows the lowest current and voltage output, indicating a direct positive correlation between operating irradiance and the overall current and voltage output of the VAA-sensitized DSSC under these conditions.

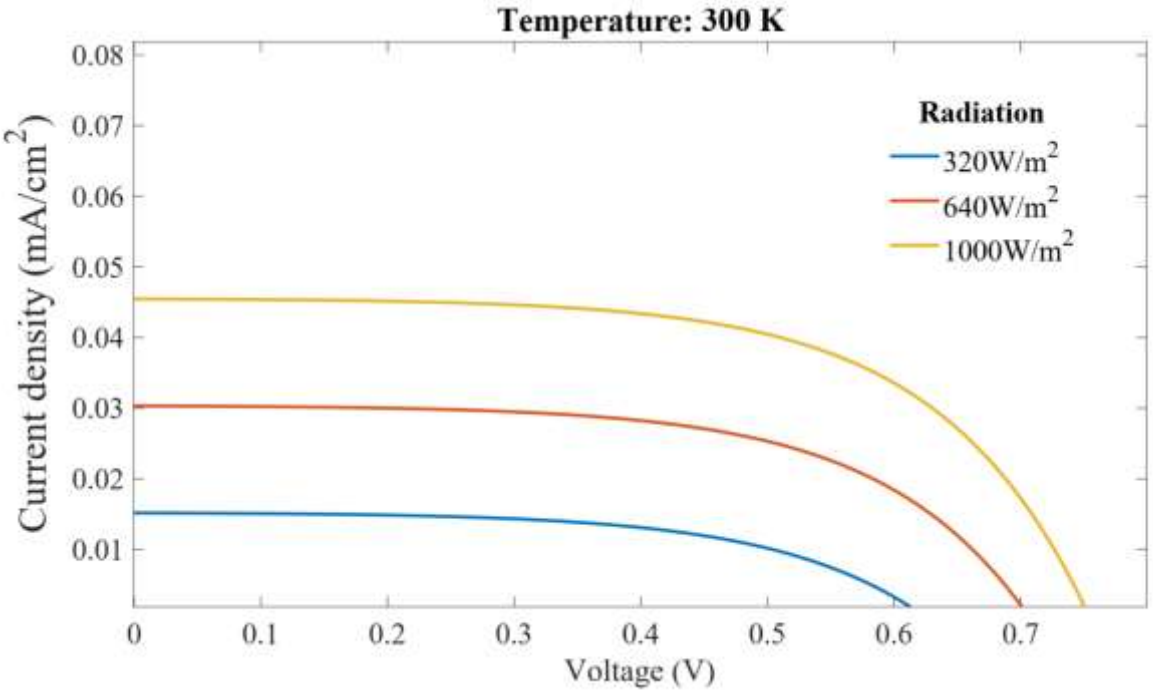

Figure 8. I-V Curve under varying solar irradiance and at a temperature of 300 K (VAA)

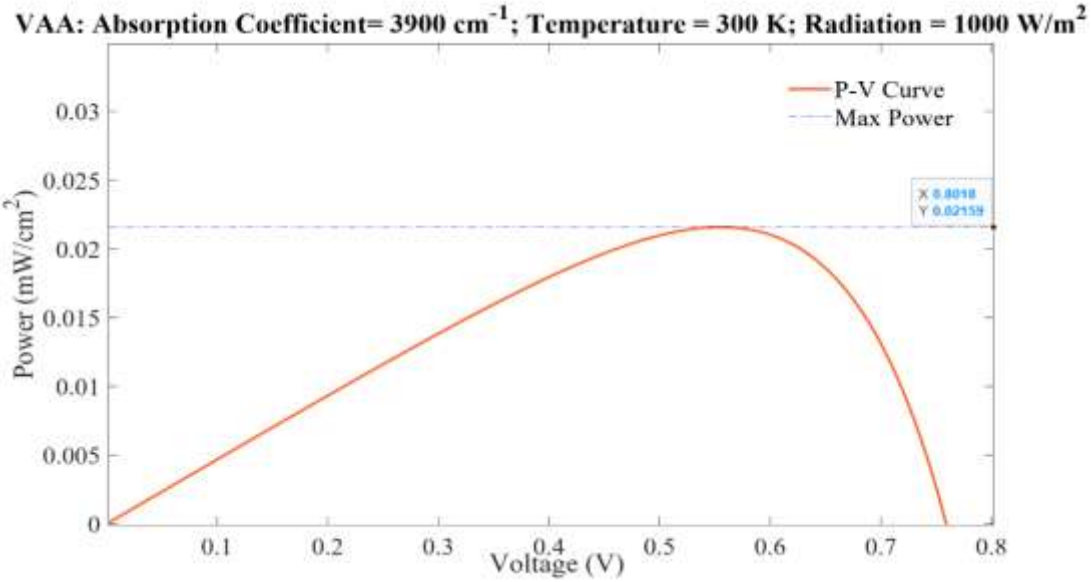

The P-V characteristics of the VAA-sensitized DSSC (Fig. 9) show a maximum power of 0.02159 mW/cm^2.

Figure 9. P-V Curve at temperature 300 K (27 °C) and at solar irradiance of 1000 W/m² (VAA)

ISSN No. 2454-6194 | DOI: 10.51584/IJRIAS |Volume XI Issue IV April 2026

Dye 2: Natural dye extract of calathea leaves (*G. macrosepala*) with acetone as solvent (GMA)

Similar to VAA dye, *G. macrosepala* (GMA) dye has absorbance peaks in the visible light region at 504, 536, 560 and 600 nm as previously reported by Soge et al. [4]. An average peak absorbance of 0.19 a.u. is considered, which falls near 550 nm in the centre of the visible light spectrum. The absorption coefficient of the solar cell is estimated as 4375 cm^{-1} using Eq. (6). The I-V curves for the GMA-sensitized DSSC under varying temperatures (Fig. 10) and irradiance (Fig. 11) show a similar trend to the VAA-sensitized DSSC, though the GMA absorption coefficient is slightly higher than that of VAA.

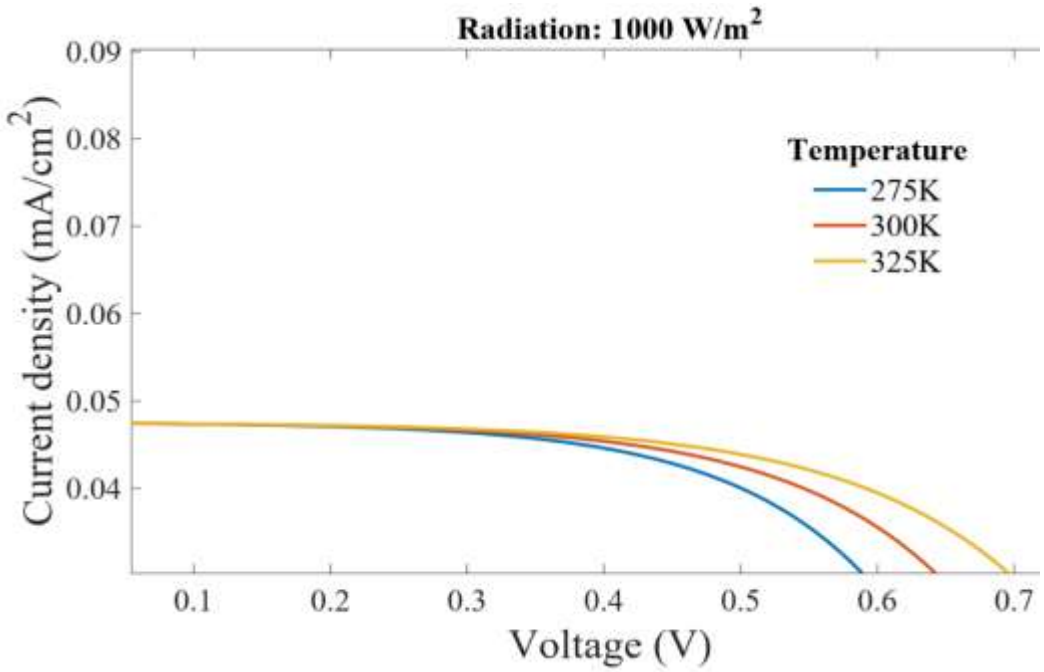

Figure 10. I-V curve under varying temperatures and at solar irradiance of 1000 W/m^2 (GMA)

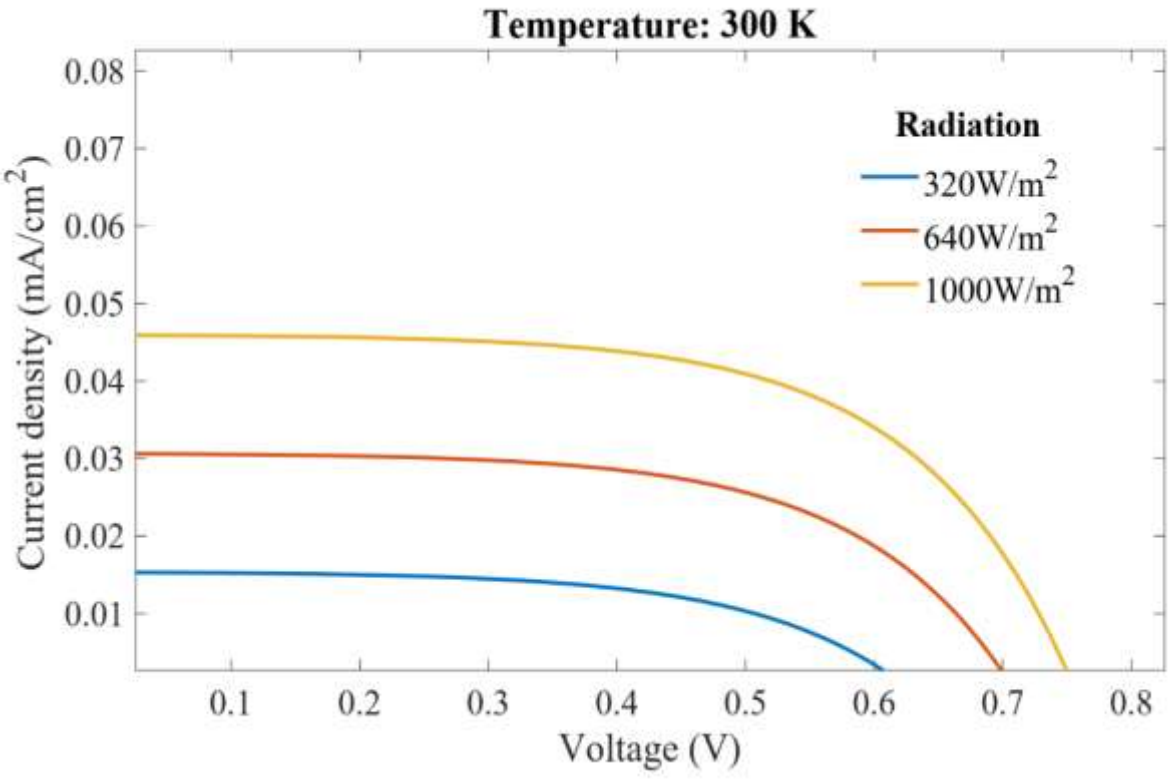

Figure 11. I-V Curve under varying solar irradiance and at temperature 300 K (GMA)

ISSN No. 2454-6194 | DOI: 10.51584/IJRIAS |Volume XI Issue IV April 2026

By observing the power-voltage (P-V) characteristics of a GMA-sensitized DSSC at a temperature of 300 K and irradiance of 1000 W/m^2 (Fig. 12), this yields a maximum power output of approximately 0.021 mW/cm^2.

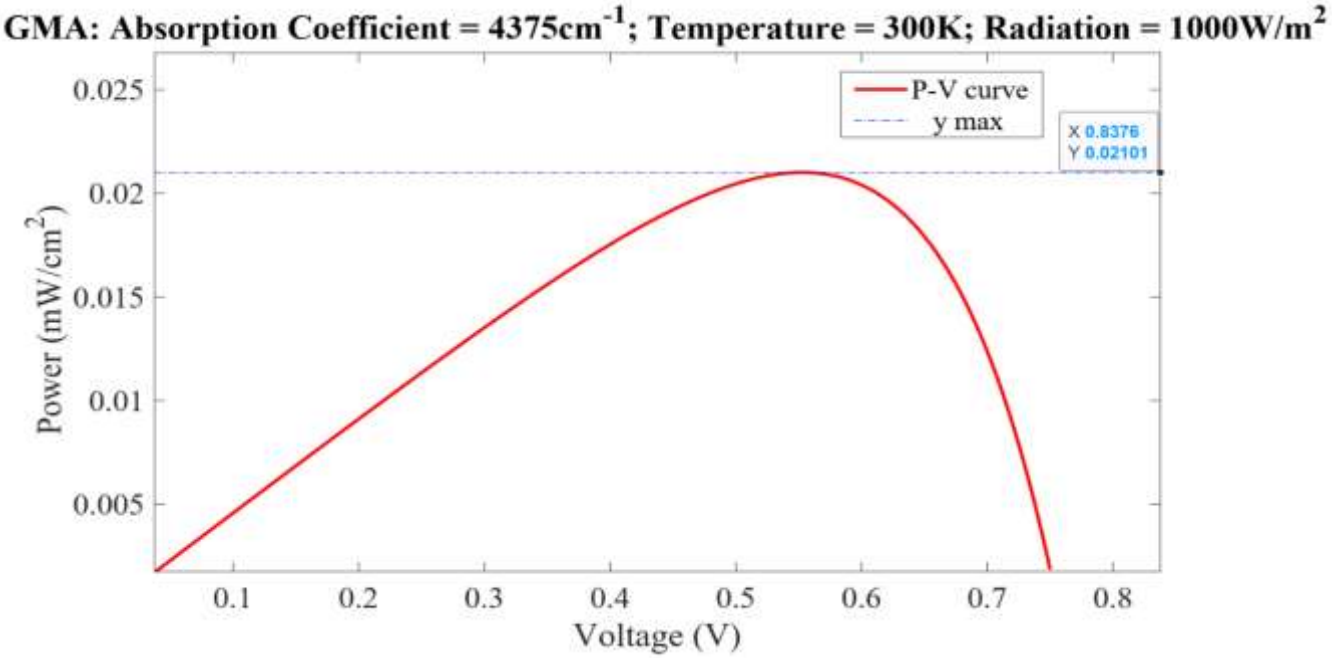

Figure 12. P-V Curve at temperature 300 K (27 °C) and at solar irradiance of 1000 W/m^2 (GMA)

Dye 3: Natural dye extract of wild alder (*C. ferruginea*) fruits (CFA)

C. ferruginea (CFA) dye has absorbance peaks in the visible light region at 504, 536, 560 and 600 nm like VAA and GMA dyes [4]. An average absorbance peak of 0.09 a.u. is considered, which lies near 550 nm in the centre of the visible light spectrum. The absorption coefficient of the solar cell is determined as 1400 cm^{-1} using Eq. (6). Figure 13 shows the current-voltage (I-V) characteristics of the CFA-sensitized DSSC with a lower absorption coefficient compared to VAA and GMA at a constant irradiance of 1000 W/m^2 across three temperatures: 275 K, 300 K, and 325 K. The curves indicate that as the temperature increases, the voltage also increases while the current remains at a stable level of approximately 0.035 mA. The curve for 325 K shows the highest voltage, while the 275 K curve shows the lowest voltage. This indicates that the voltage increases with increasing temperature as expected.

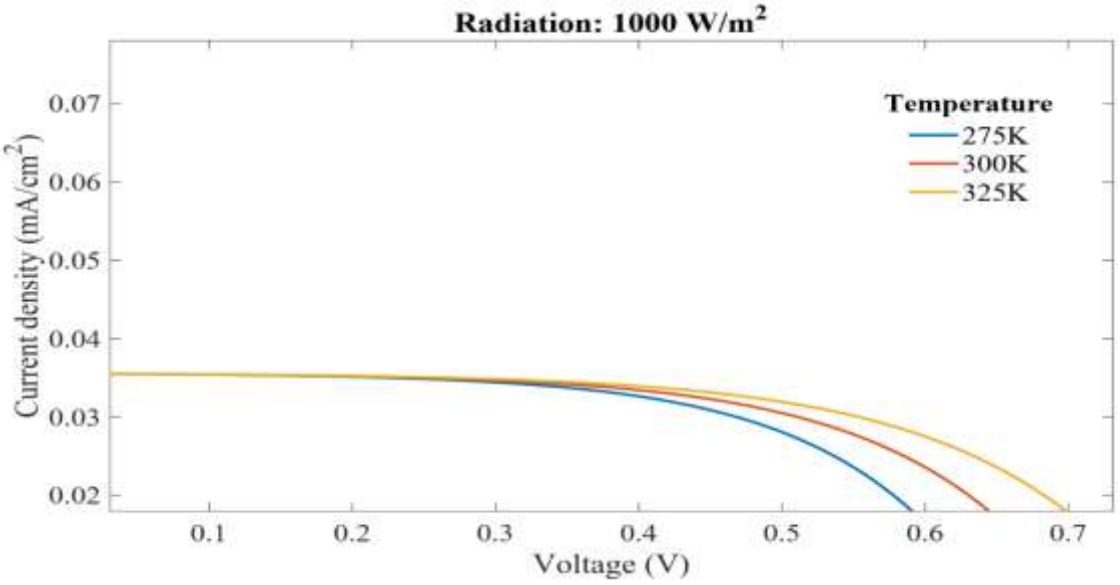

Figure 13. I-V Curve under varying temperatures and at solar irradiance of 1000 W/m^2 (CFA)

ISSN No. 2454-6194 | DOI: 10.51584/IJRIAS |Volume XI Issue IV April 2026

In Fig. 14, while there is a slight increase in the voltage as the irradiance increases, there is a significant increase in the current, with the highest current yield of 0.035 A at 1000 W/m^2. We can conclude that solar irradiance plays a crucial role in increasing the current. Additionally, an increase in temperature is associated with an increase in voltage. The highest result was achieved at solar irradiance of 1000 W/m^2 and a temperature of 300 K, as there is only a slight increase in voltage with an increase in irradiance.

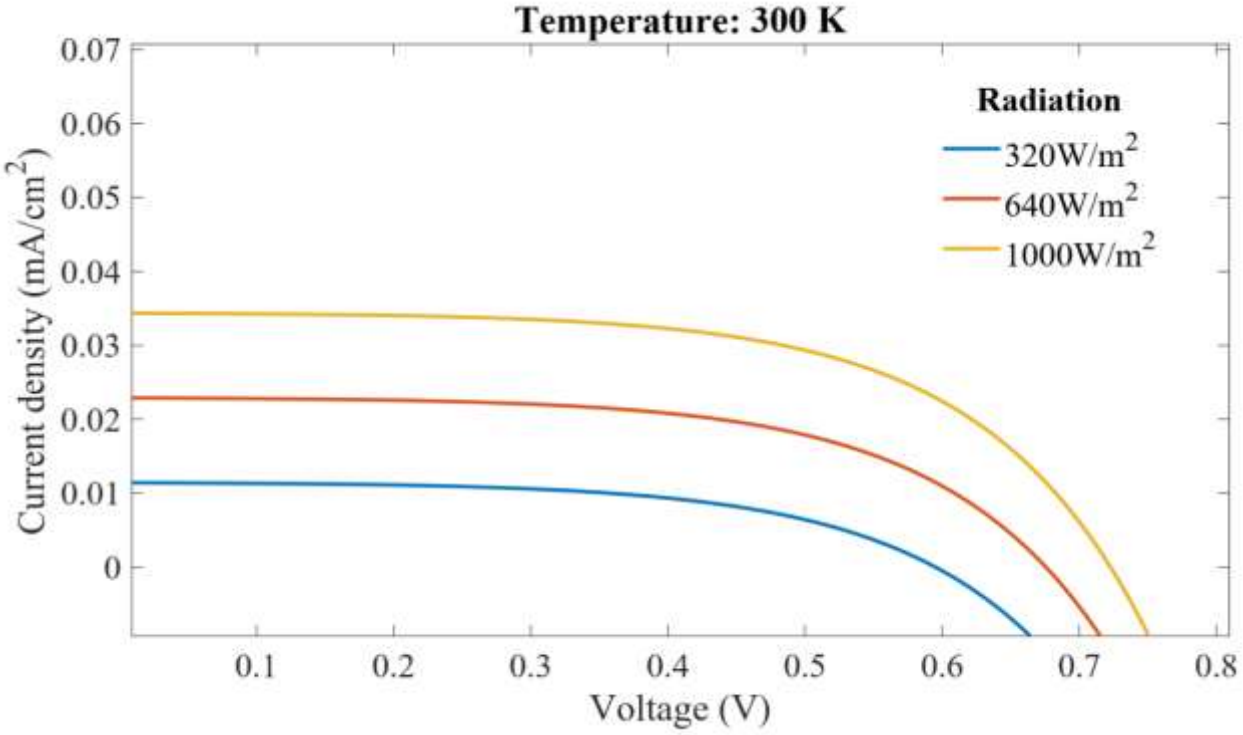

Figure 14. I-V Curve under varying solar irradiance at temperature 300 K (CFA)

As illustrated in Fig. 15, CFA dye yields a lower maximum power of 0.0148 mW/cm^2 compared to other dyes because of its low absorption coefficient.

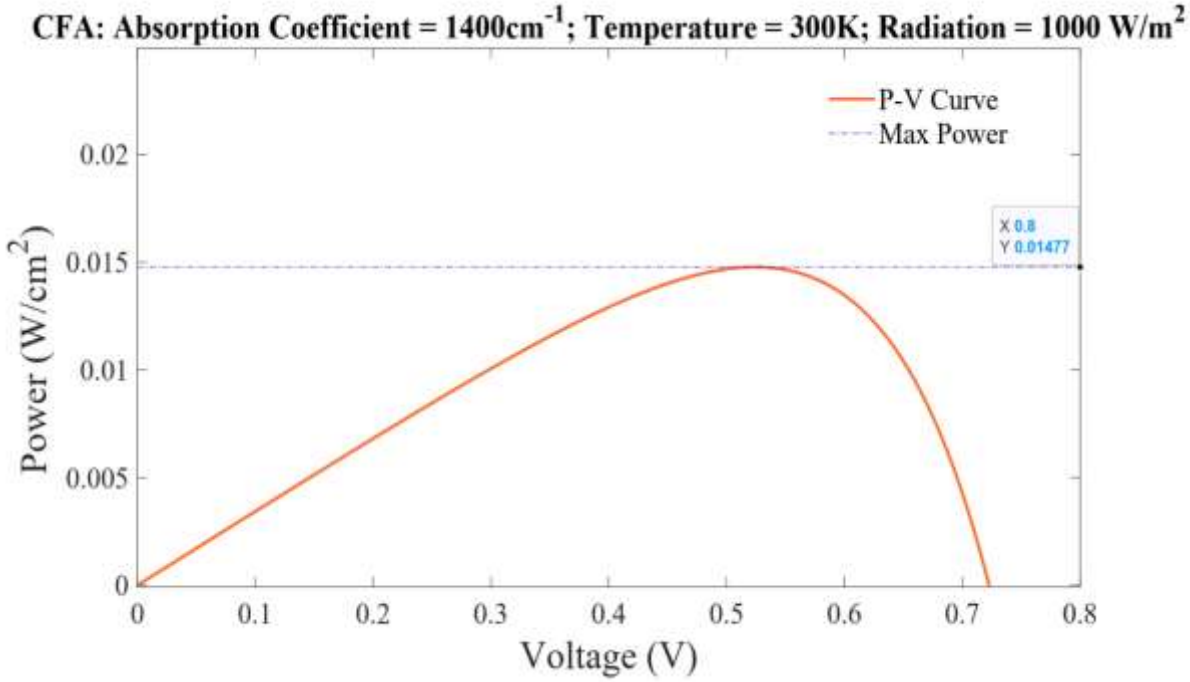

Figure 15. P-V Curve at temperature 300 K (27 °C), solar irradiance 1000 W/m^2, and absorption coefficient 1400 cm^{-1} (CFA)

ISSN No. 2454-6194 | DOI: 10.51584/IJRIAS |Volume XI Issue IV April 2026

Analysis of the three dyes (VAA, GMA, CFA)

A combined I-V curve of the three dyes is displayed in Fig. 16 to reveal the varying changes in the characteristics of the DSSC cell for each dye at 1000 W/m² and at 300 K (27 °C).

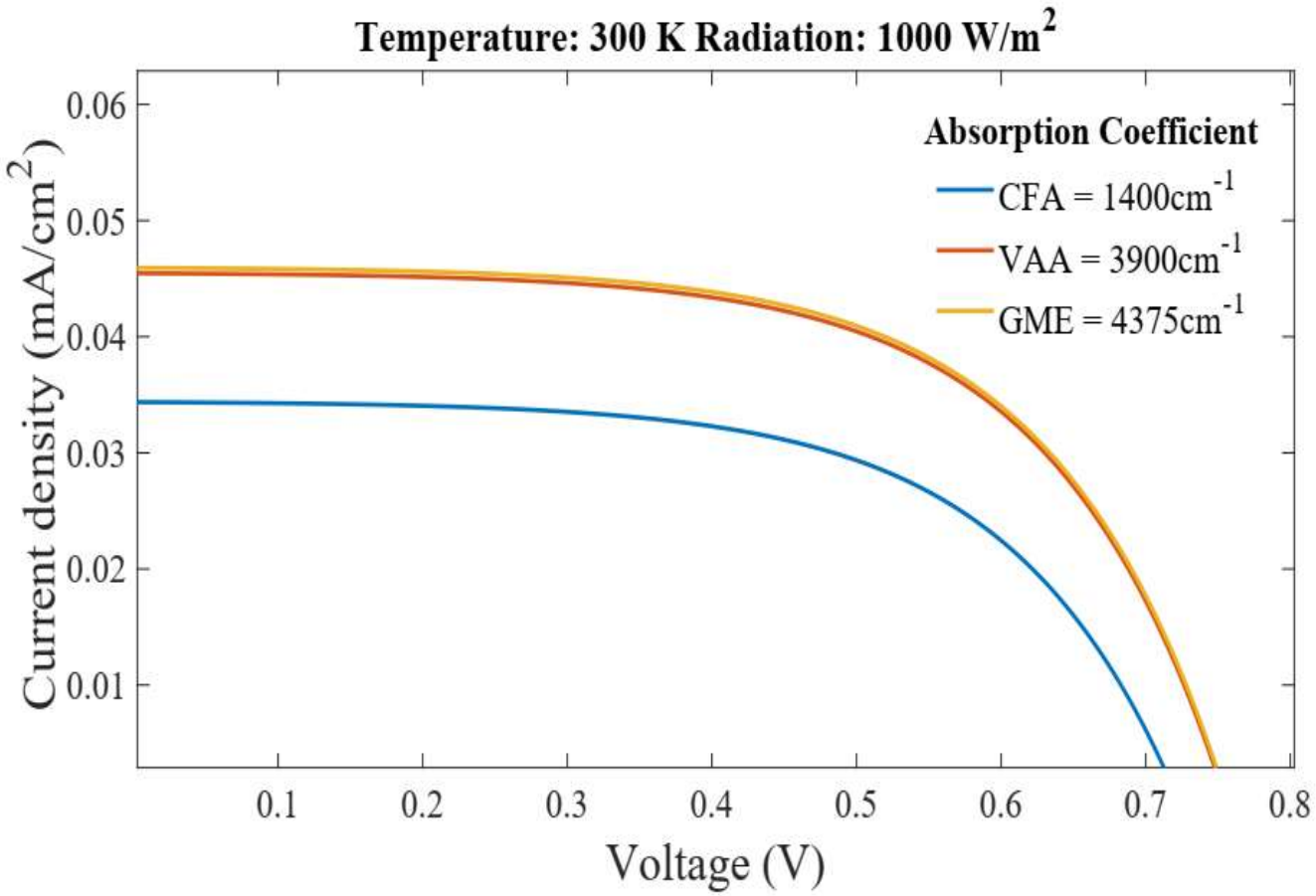

Figure 16. I-V Curve of the three dyes at temperature 300 K and solar irradiance 1000 W/m²

Figure 16 clearly illustrates how the absorption coefficient of each dye significantly affects the current output, with only a slight variation in the voltage across each cell. This indicates that an increased absorption coefficient in the visible light region, between 500 nm and 600 nm, results in a higher short-circuit current, and optimizing these characteristics of the dyes is vital for efficient light harvesting.

Modelled GMA DSSC Cell

The PV and IV characteristics of the DSSC cell that produced the highest absorption coefficient of 4375 cm^{-1} (GMA) were modelled as illustrated in Fig. 17. The fill factor (FF) was calculated from the values of the maximum power P_{mp}, open-circuit voltage V_{OC}, and short-circuit current $I_{SC,}$ as expressed by Eq. (7).

$$FF = \frac{P_{mp}}{I_{sc} \times V_{oc}} = \frac{0.0218}{0.048 \times 0.76} = 0.598 \approx 0.6 \quad (7)$$

ISSN No. 2454-6194 | DOI: 10.51584/IJRIAS |Volume XI Issue IV April 2026

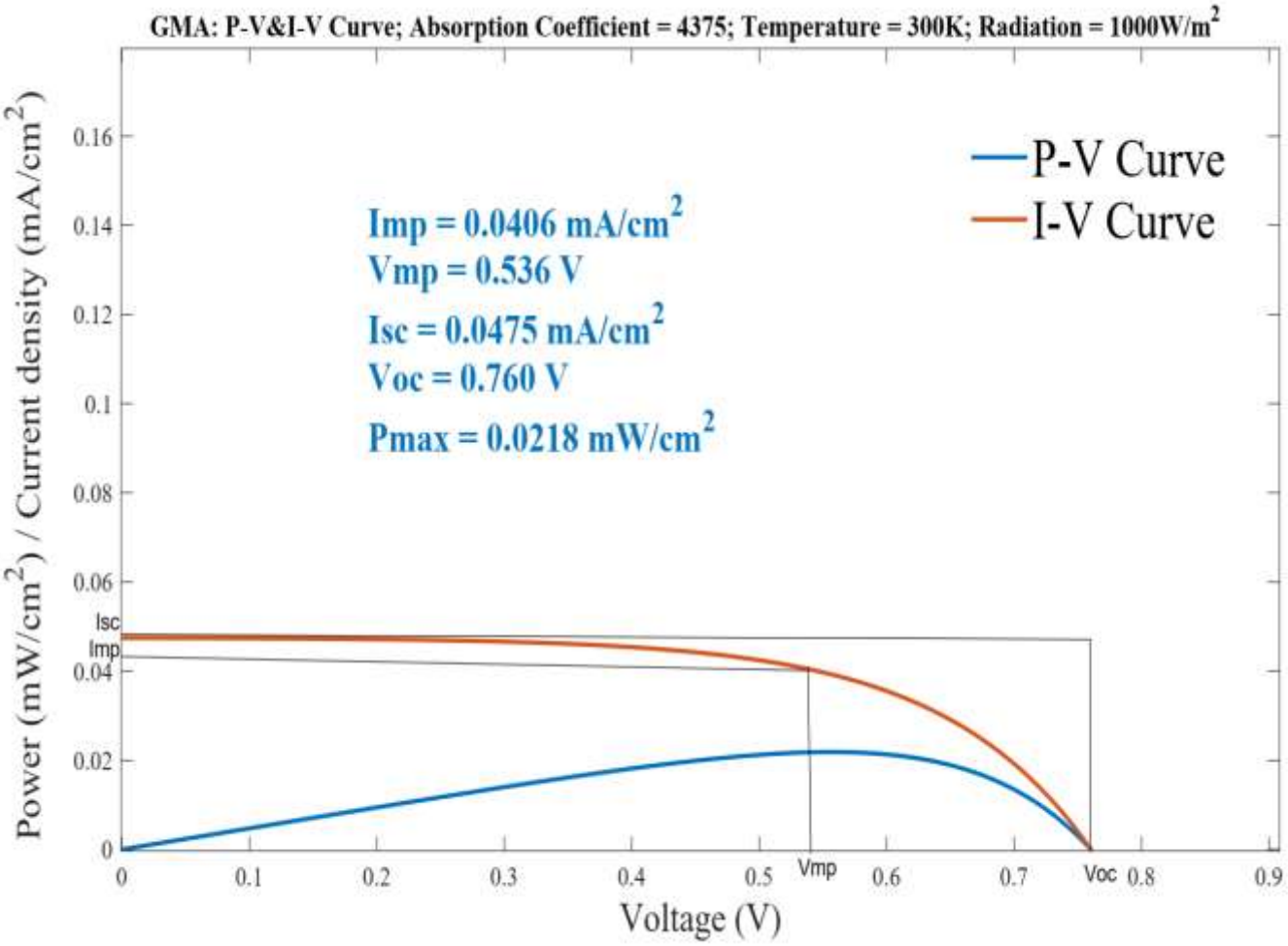

Figure 17. I-V and P-V Curve of GMA showing detailed values at temperature 300K and solar irradiance 1000 W/m²

The efficiency of the cell was calculated using the formula for efficiency. Since the irradiance is 1000 W/m², the power input (P_{in}) was converted to 100 mW/cm² for each cell of 0.36 cm². An efficiency of approximately 0.02% was derived using Eq. (8).

$$\eta = \frac{P_{max}}{P_{in}} \times 100\% = \frac{0.0218}{100} \times 100\% = 0.02\% \quad (8)$$

Furthermore, a DSSC solar panel modelled with 500 GMA-Sensitized DSSCs in series – ten cells are connected in series and fifty series-strings are connected in parallel. The maximum power at peak working conditions was calculated by multiplying the number of cells by the maximum power (P_{max}) of each cell. The electrical characteristics of the modelled solar panel are estimated below:

- Maximum Power: 10.9 mWp (Watt-peak) (≈ 0.01 Wp)

$$P_{MP} = 500 \times 0.0218\, mW = 10.9\, mW \approx 0.01\, Wp \quad (9)$$

- Voltage at Max Power (V_{MP}): 5.36 V (1000 W/m², 27°C)

$$V_{MP} = N_S \times Voc = 10 \times 0.536 = 5.36\, V \quad (10)$$

ISSN No. 2454-6194 | DOI: 10.51584/IJRIAS |Volume XI Issue IV April 2026

where N_s is the number of solar cells in series.

- Current at Max Power (Imp): 20.3 mA

$$I_{MP} = N_P \times I_{mp} = 500 \times 0.0406 = 20.3\, mA \quad (11)$$

where N_p is the number of solar cells in parallel

- Open-Circuit Voltage (V_{OC}): 7.6 V

$$V_{OC} = N_S \times V_{oc} = 10 \times 0.76 = 7.6\, V \quad (12)$$

- Short-Circuit Current (I_{SC}): 23.75 mA

$$I_{SC} = N_P \times I_{sc} = 500 \times 0.045 = 23.75\, mA \quad (13)$$

Number of solar cells: 500 DSSCs with 0.36-cm^2 active cell area.

- Arrangement: ten cells are connected in series, and fifty-series strings are connected in parallel.

E. Comparison with Experimentally Validated Results

The simulated results were compared to those of the DSSCs fabricated using natural dyes as photosensitizers, with an active cell area of 0.36 cm^2 and characterised using simulated sunlight of a solar simulator at 1000 W/m^2 (FY700 Solar Simulator; FY Tronix Electronic) as presented in Table 3. The fabrication process and electrical characterisation of the solar cells have been reported by Soge et al. [4].

Table 3. Comparison of Experimental Results and Simulation Results

Dyes	Experimental Results				Simulation Results			
	I_{SC} (mA/cm^2)	V_{OC} (V)	η (%)	FF	I_{SC} (mA/cm^2)	V_{OC} (V)	η (%)	FF
VAA	0.119	0.522	12×10^{-2}	0.7	0.0470	0.754	2×10^{-2}	0.6
GMA	0.075	0.512	7×10^{-2}	0.6	0.0475	0.760	2×10^{-2}	0.6
CFA	0.044	0.522	4×10^{-2}	0.6	0.0345	0.710	1.5×10^{-2}	0.6

The open-circuit voltage (V_{OC}) of the simulated result is similar to that of the experimental result, and only a difference of approximately 0.2 V was observed. This observation in the experimental results could be attributed to a lower temperature and a higher thickness value of the TiO_2 layer, which leads to an increase in the resistance of the DSSC, resulting in a drop in the voltage output. The fill factor of the simulated results is consistent with that of the experimental results, except for that of VAA, which is 0.6 in the simulated result and 0.7 in the experimental result. The efficiency of the cells is of the same order for both simulated and experimental results.

These results validate the accuracy of the MATLAB/Simulink model and its application for the prediction of the electrical performance of DSSCs sensitized with natural dye.

Furthermore, according to Soge et al. [4], the low efficiencies of the three natural dyes are due to their inherent challenges, such as narrow absorption spectra attributed to their less optimized molecular structures, poor photostability under prolonged illumination, slow electron injection rates, and high recombination losses. The slow electron injection rates are traceable to poor alignment of the highest occupied molecular orbital (HOMO) and lowest unoccupied molecular orbital (LUMO) of the dye which play critical roles in determining the power conversion efficiency of the DSSC. However, optimization of the DSSC performance is achievable through proper molecular engineering of the natural dyes to tune the HOMO and LUMO levels.

Moreover, the novelty and contribution of this study are highlighted below:

1. The novelty of this study is the design of a functional DSSC panel, bridging the gap between simulation and real-world implementation.
2. The use of natural dye extracts of *G. macrosepala*, *V. amygdalina*, and *C. ferruginea* as photosensitizers in the modelling and simulation of the electrical properties of DSSCs contributed towards sustainable energy research.

CONCLUSION

An equivalent MATLAB/Simulink model was developed to simulate the electrical properties of DSSCs using three natural dye extracts. A detailed single-diode equivalent circuit model was constructed in MATLAB/Simulink, accurately reflecting the complex electrochemical dynamics of DSSCs. This model was used to simulate the I-V and P-V characteristics of DSSCs sensitized with specific natural dyes across various temperatures and solar irradiance levels. Simulation results indicated that temperature positively influenced the open-circuit voltage (V_{OC}) while the short-circuit current (I_{SC}) exhibited minimal variation. Conversely, increased solar irradiance significantly enhanced I_{SC} and also elevated V_{OC}. Among the three natural dyes, *G. macrosepala* and *V. amygdalina*, with higher absorption coefficients, demonstrated superior current and power generation compared to *C. ferruginea*. The simulation outcomes were validated against experimental data, showing consistency. The model's practicality was evidenced by the design of a functional DSSC solar panel comprising 500 GMA-sensitized cells with 0.36-cm^2 active cell area. The model estimated a panel output of approximately 10.9 mWp, with a maximum current and voltage of 20.3 mA and 5.36 V recorded, respectively. In conclusion, this work provides a versatile simulation framework for natural dye-sensitized solar cells, offering valuable insights into their performance under varying environmental conditions and aiding the preliminary design of functional DSSC solar panels. Further work will include artificial intelligence (AI) integration or advanced materials to align with emerging trends in DSSC modelling and optimization.

REFERENCES

1. M. Grätzel, “Photoelectrochemical cells,” Nature, vol. 414, no. 6861, pp. 338–344, 2001.
2. K. Sharma, V. Sharma, and S. S. Sharma, “Dye-sensitized solar cells: Fundamentals and current status,” Nanoscale Research Letters, vol. 13, no. 1, p. 381, 2018.
3. M. I. Khan, H. Ullah, M. A. Khan, and A. Khan, “Recent advancements in dye-sensitized solar cells: A review of sensitizers, electrolytes, and photoelectrodes,” Journal of Energy Storage, vol. 71, p. 108147, 2023.
4. A. Soge, A. Oshin, C. Ulbricht, F. Mayr, O. Olukanni, O. Dairo, M. Sanyaolu, O. Adeyemi, S. Tekoglu, M. Scharber, and A. Willoughby, “Comparative study of dye-sensitized solar cells with natural dye extracts of Vernonia amygdalina, Goeppertia macrosepala leaves, and Cnestis ferruginea fruit as photosensitizers,” Journal of Electronic Materials, vol. 54, no. 10, pp. 8628–8642, 2025.
5. A. Hagfeldt, G. Boschloo, L. Sun, L. Kloo, and H. Pettersson, “Dye-sensitized solar cells,” Chemical Reviews, vol. 110, no. 11, pp. 6595–6663, 2010.
6. A. S. Al-Ezzi and M. N. M. Ansari, “Photovoltaic solar cells: A review,” Applied System Innovation, vol. 5, no. 4, p. 67, 2022.
7. Y. Mallal, D. K. Sharma, L. El Bahir, and T. Hassboun, “Temperature prediction-based realistic performance analysis of various electrical configurations of solar PV panels,” Solar Energy, vol. 219, pp. 19–28, 2021.

8. A. M. Farayola, "Solar cell parameter extraction and power optimization in photovoltaic systems," 2023.
9. A. Carella, F. Borbone, and R. Centore, "Research progress on photosensitizers for DSSC," Frontiers in Chemistry, vol. 6, p. 481, 2018.
10. K. Snimaetsya, "Equivalent circuit modeling of dye-sensitized solar cells: A review of recent advances," Renewable and Sustainable Energy Reviews, vol. 135, p. 110149, 2021.
11. Y. Mallal, D. K. Sharma, L. El Bahir, and T. Hassboun, "Temperature prediction-based realistic performance analysis of various electrical configurations of solar PV panel," Solar Energy, vol. 219, pp. 19–28, 2021.
12. P. K. Olulope, A. O. Adeleye, and A. B. Amomoh, "Design and simulation of dye sensitized solar cell as a cost-effective alternative to silicon solar panel," Scientific Review, vol. 4, no. 5, pp. 44–52, 2018.
13. J. Kaur, G. Pandey, and R. Kumar, "Design and performance analysis of dye sensitized solar cell using MATLAB/Simulink," Materials Today: Proceedings, vol. 46, pp. 10419–10423, 2021.
14. A. Islam, M. Z. Yahya, and A. A. Umar, "Modeling and simulation of natural dye sensitized solar cell using diffusion model in MATLAB," Materials Today: Proceedings, vol. 46, pp. 10419–10423, 2021.
15. A. Sahu, D. Bhatia, and S. Kaur, "Machine learning applications in photovoltaic energy systems: A DSSC focus," Energy AI, vol. 12, p. 100203, 2023.
16. B. Yadagiri, A. K. Kaliamurthy, K. Yoo, H. C. Kang, J. Ryu, F. K. Asiam, and J. Lee, "Molecular engineering of photosensitizers for solid-state dye-sensitized solar cells: Recent developments and perspectives," ChemistryOpen, vol. 12, no. 12, 2023.
17. B. O'Regan and M. Grätzel, "A low-cost, high-efficiency solar cell based on dye-sensitized colloidal TiO2 films," Nature, vol. 353, no. 6346, pp. 737–740, 1991.
18. D. M. Atia and N. M. Ahmed, "Mathematical modeling, parameter identification, and electrical performance of a DSSC based on nature-inspired optimization techniques," Journal of Computational Electronics, vol. 22, no. 2, pp. 723–741, 2023.
19. A. M. Tayeb, A. A. A. Solyman, and M. Hassan, "Modeling and simulation of dye-sensitized solar cell: Model verification for different semiconductors and dyes," Alexandria Engineering Journal, vol. 61, no. 11, pp. 8643–8654, 2022.
20. A. Aboulouard, S. Rbihi, Y. Najih, M. Adar, A. Jouaiti, B. Elhadadi, and M. A. El Abbassi, "Numerical simulation of dye-sensitized solar cells performance for local natural dyes," in IEEE 6th International Conference on Optimization, 2020.
21. L. Arumugam, P. L. Low, M. E. Yeoh, G. Thien, Y. K. Sin, and K. Y. Chan, "Simulation of dye-sensitized solar cell with mesoporous zinc oxide layer of different thicknesses and with dye-sensitisers of different absorption coefficients," in MECON, vol. AER 214, pp. 315–333, 2022.
22. Z. Tajvar, S. M. Faraz, Z. H. Awan, and M. H. Sayyad, "Modelling and simulation of eco-friendly solar cells sensitized by natural dyes," Energy & Environment, vol. 35, no. 1, pp. 275–288, 2022.
23. C. O. Ogabi, B. A. Idowu, A. O. Boyo, S. O. Oseni, and R. O. Kesinro, "Simulation and performance of natural sensitizer dye from Lagerstroemia speciosa flowers and leaves," Journal of Materials Science Research and Reviews, vol. 4, no. 1, pp. 60–65, 2021.
24. S. Roy and A. K. Srivastava, "Numerical simulation of dye-sensitized solar cell performance using finite element method," Solar Energy, vol. 205, pp. 357–366, 2020.
25. E. Supriyanto, H. A. Kartikasari, N. Alviati, and G. Wiranto, "Simulation of dye-sensitized solar cells (DSSC) performance for various local natural dye photosensitizers," IOP Conference Series: Materials Science and Engineering, vol. 515, p. 012048, 2019.
26. A. Razvitia, "Dye-sensitized solar cells: Materials, devices, and future perspectives," Renewable and Sustainable Energy Reviews, vol. 113, p. 109286, 2019.
27. A. Razvitia, "Natural dyes for dye-sensitized solar cells: A review of sources, extraction, and performance," Renewable and Sustainable Energy Reviews, vol. 141, p. 110806, 2021.
28. V. Predstavleno, "Porphyrin-based dyes for dye-sensitized solar cells: A review of molecular design and photovoltaic performance," Coordination Chemistry Reviews, vol. 408, p. 213184, 2020.
29. A. O. Salau, A. S. Olufemi, G. Oluleye, V. A. Owoeye, and I. Ismail, "Modeling and performance analysis of dye-sensitized solar cell based on ZnO compact layer and TiO2 photoanode," Materials Today: Proceedings, vol. 51, pp. 502–507, 2021.

ISSN No. 2454-6194 | DOI: 10.51584/IJRIAS |Volume XI Issue IV April 2026

30. O. Dubey and R. Ganguly, “A comprehensive device modeling of solid-state dye-sensitized solar cell by MATLAB,” International Journal of Research in Engineering, Science and Management, vol. 3, no. 11, pp. 324–328, 2020.
31. D. Kumar, K. P. S. Parmar, and P. Kuchhal, “Optimizing photovoltaic efficiency of a dye-sensitized solar cell (DSSC) by a combined (modelling-simulation and experimental) study,” International Journal of Renewable Energy Research, vol. 10, no. 1, p. 165, 2020.